

Nonlinear optical properties of silicon nanocrystals grown by plasma-enhanced chemical vapor deposition

G. Vijaya Prakash,^{a)} M. Cazzanelli, Z. Gaburro, and L. Pavesi
INFN and Dipartimento di Fisica, Università di Trento, via Sommarive 14, 38050 Povo, 38100 Trento, Italy

F. Iacona
CNR-IMETEM, Stradale Primosole 50, 95121 Catania, Italy

G. Franzò and F. Priolo
INFN and Dipartimento di Fisica, Università di Catania, Corso Italia 57, 95129 Catania, Italy

(Received 8 October 2001; accepted for publication 4 January 2002)

The real and imaginary parts of third-order nonlinear susceptibility $\chi^{(3)}$ have been measured for silicon nanocrystals embedded in SiO_2 matrix, formed by high temperature annealing of SiO_x films prepared by plasma-enhanced chemical vapor deposition. Measurements have been performed using a femtosecond Ti-sapphire laser at 813 nm using the Z-scan technique with maximum peak intensities up to $2 \times 10^{10} \text{ W/cm}^2$. The real part of $\chi^{(3)}$ shows positive nonlinearity for all samples. Intensity-dependent nonlinear absorption is observed and attributed to two-photon absorption processes. The absolute value of $\chi^{(3)}$ is on the order of 10^{-9} esu and shows a systematic increase as the silicon nanocrystalline size decreases. This is due to quantum confinement effects. © 2002 American Institute of Physics. [DOI: 10.1063/1.1456241]

Since the discovery of efficient visible emission from porous Si,¹ silicon nanocrystals (Si-nc) have been studied extensively.² Besides its intense visible emission, Si-nc are also promising materials for nonlinear optical applications.³ Many authors have studied the nonlinear optical properties of Si-nc by using porous Si.⁴ However, there is a need for a more specific study on the nonlinear optical properties of well-defined systems. Earlier literature reports on nonlinear optical properties of Si-nc show a large scatter in the data due mainly to inhomogeneous samples where broad size distribution causes an intensity-dependent interaction between Si-nc and no reliable study as a function of nanocrystal size was possible.⁵⁻⁷ A controlled production of Si-nc, particularly referring to the dimension and the size distribution, is thus necessary to relate the nonlinear optical properties to the quantum confinement effect. Plasma-enhanced chemical vapor deposition (PECVD) is one of the most versatile techniques for growing Si-nc. In recent publications we presented an extensive study of the structural, optical, x-ray absorption fine structure and theoretical investigations of this system.⁸⁻¹⁰ In this article, we report on the measurements of sign and magnitude of both real and imaginary parts of third-order nonlinear susceptibility $\chi^{(3)}$ of Si-nc grown by PECVD by the Z-scan method as a function of Si-nc sizes.

The SiO_x films were prepared by using a parallel plate PECVD system. The experimental procedure is reported elsewhere.^{9,10} These films were deposited on a quartz substrate in a three layers waveguide geometry, where two 100 nm thick SiO_2 films sandwiched a 230 nm thick SiO_x layer. An error of 10% can be estimated on the thickness of the films. High temperature annealing of SiO_x films induces

phase separation as Si and SiO_2 and as a consequence, Si-nc are formed.⁹ The Si-nc size depends on the excess Si amount as well as on the annealing temperature. Si contents, obtained from Rutherford backscattering spectrometry (RBS) measurements, Si-nc radius obtained from transmission electron microscopy (TEM), and annealing temperatures for the three representative samples investigated here are given in Table I.

Z-scan experiments^{11,12} were performed on these samples by using a Gaussian laser beam (Ti:sapphire laser, wavelength $\lambda = 813 \text{ nm}$ with a repetition rate of 82 MHz and with 60 fs pulse width) in a tight focus limiting geometry. The beam waist at the focus of the lens is typically $19 \mu\text{m}$ with peak intensity up to $2 \times 10^{10} \text{ W/cm}^2$. This was varied by using neutral density filters. The sample is moved along the optical path by a computer driven continuous motor. The sample transmission is monitored by a silicon photodiode (D1). An aperture is placed in front of D1 for closed aperture measurements. A small part of the input intensity is monitored by another photodiode (D2) and the ratio (D1/D2) is recorded as a function of the sample position z . The experimental setup was checked by measuring a reference sample CS_2 .¹¹⁻¹³ The transmission with and without the aperture was measured in the far field as the sample moved through the focal point, enabling the separation of the nonlinear refractive index from the nonlinear absorption. No dependence on repetition rates, even for frequency down to 100 Hz, was observed. Moreover, during the 3 h long experiment, we did not observe any changes in the Z scan trace. Thermal effects are hence negligible in our measurements.¹⁴

The normalized transmission of closed aperture (finite aperture at the far field) Z scan is given by^{5,11}

^{a)} Author to whom correspondence should be addressed; electronic mail: gaddam@science.unitn.it

TABLE I. Si content (obtained from RBS measurements), temperatures of thermal treatment, Si-nc radius estimated from TEM where within parenthesis is reported the width of the radius distribution, real ($\text{Re } \chi^{(3)}$) and imaginary ($\text{Im } \chi^{(3)}$) parts of third-order nonlinear susceptibilities, nonlinear absorption coefficients (β), and absolute third-order nonlinear susceptibilities ($\chi^{(3)}$) (at peak intensity of $4\text{GW}/\text{cm}^2$).

Sample	Si content/ thermal treatment	Si-nc radius (nm)	$\text{Re } \chi^{(3)}$ (esu) $\times 10^{-9}$	β (m/GW)	$\text{Im } \chi^{(3)}$ (esu) $\times 10^{-10}$	$\chi^{(3)}$ (esu)
5C	39 at. %/1100 °C	<0.7	$+3.8 \pm 0.8$	0.2 ± 0.03	0.3 ± 0.06	3.8×10^{-9}
1C	46 at. %/1100 °C	1.0(0.5)	$+1.9 \pm 0.4$	1.4 ± 0.3	2.1 ± 0.4	1.9×10^{-9}
5A	39 at. %/1250 °C	1.5(0.7)	$+1.3 \pm 0.2$	0.4 ± 0.07	0.6 ± 0.09	1.3×10^{-9}

$$T(z) = 1 + \frac{4x\Delta\phi}{(x^2+9)(x^2+1)}, \quad (1)$$

where $x = z/z_0$, z is the longitudinal distance from the focal point, z_0 is the Rayleigh range of the beam, and $\Delta\phi$ is the nonlinear phase change. The normalized closed aperture Z scan data are fitted with Eq. (1) to obtain $\Delta\phi$ values. The nonlinear index of refraction γ is then related to $\Delta\phi$ by

$$\gamma = \frac{\Delta\phi\lambda\alpha}{2\pi I_0(1 - e^{-\alpha l})}, \quad (2)$$

where α is the linear absorption coefficient at 813 nm and l is the thickness of the SiO_x layer, I_0 is the peak intensity at the focus, and λ is the wavelength of the pump laser. The closed Z-scan data for sample 5A is given in Fig. 1. The experiments were also performed on the pure quartz substrate and no significant contribution from the quartz substrate was found. The closed aperture data for all the samples show a distinct valley-peak configuration typical of positive nonlinear effects (self focusing), as expected for most of the dispersive materials.^{4,6,11,15,17,19} The real part of the third-order

nonlinear susceptibility is obtained from $\text{Re } \chi^{(3)} = 2n^2\epsilon_0 c \gamma$ (see Table I), where n is the linear refractive index, ϵ_0 is the permittivity of free space, and c is the velocity of light. The effective refractive index n is considered to be 1.7, obtained from m -line measurements on these samples.

Figure 2 shows the normalized open aperture transmission (full power into the detector) as a function of z for sample 5A. A symmetric inverted bell shaped transmission is measured with a minimum at the focus ($z=0$). When direct absorption is negligible, one can deduce the nonlinear absorption coefficient β from the open aperture Z-scan data. For a thin sample of thickness l^5

$$T(z) = 1 + \frac{\beta I_0 l}{\left(1 + \frac{z^2}{z_0^2}\right)}. \quad (3)$$

The open aperture experiment is done for repeated times and for different peak intensities between $0.3\text{--}2 \times 10^{10} \text{ W}/\text{cm}^2$ to ensure proper measurements. The results for various samples are reported in Table I. On comparison,

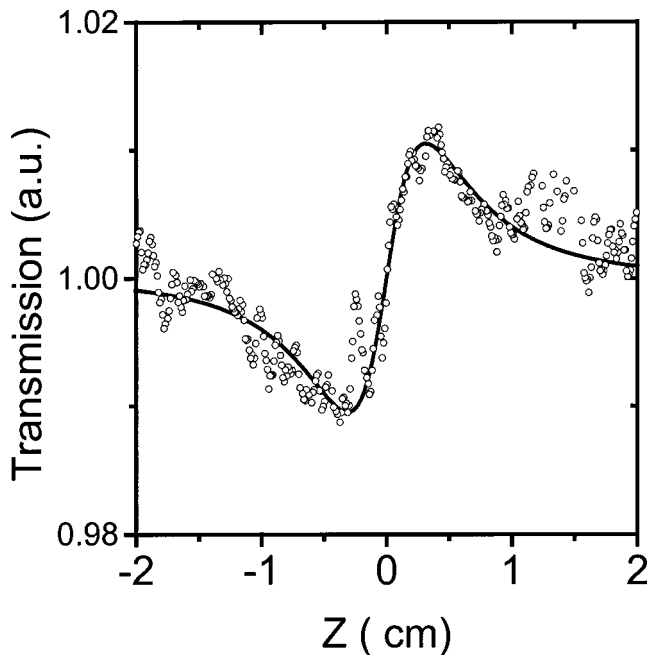


FIG. 1. Closed aperture Z-scan data for sample 5A (Si content 39 at. % with thermal treatment at 1250 °C) at the peak intensity of $3.9 \text{ GW}/\text{cm}^2$. Solid line is the experimental fit using Eq. (1).

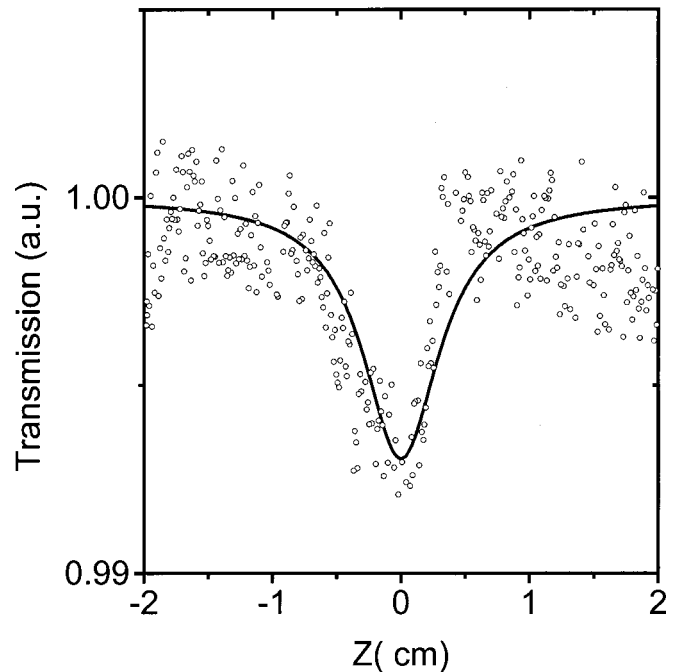


FIG. 2. Open aperture Z-scan data for sample 5A (Si content 39 at. % with thermal treatment at 1250 °C) at peak intensity $7.5 \text{ GW}/\text{cm}^2$. Solid line is the experimental fit using Eq. (3).

the β values we measured are higher than the value of crystalline silicon (*c*-Si)^{16,17} and close to the values for porous silicon⁴ (see Table I). The present values are enhanced more by 2 orders of magnitude than the theoretically predicted nonlinear absorption coefficients for *c*-Si.¹⁷ Knowing β , the imaginary part of the third-order nonlinear susceptibility $\chi^{(3)}$ is evaluated by

$$\text{Im } \chi^{(3)} = \frac{n^2 \epsilon_0 c \lambda \beta}{2\pi}$$

The nonlinear absorption in most of the refractive materials arises from either direct multiphoton absorption or saturation of single photon absorption.^{11,14} Z-scan traces with no aperture are expected to be symmetric with respect to the focus ($Z=0$) where they have the minimum transmittance (for two or multiphoton absorption) or maximum transmittance (for saturation of absorption). It is interesting to note that the nonlinear absorption in Si-nc formed by ion implantation and laser ablation is selective to the excitation as well as cluster size.^{5,6,21,22} For example, laser ablated samples exhibit saturation of absorption and bleaching effects (change of sign for nonlinear absorption from positive to negative with the increase of pump intensity) at the near resonant excitations (355 and 532 nm).²¹ In contrast, ion implanted samples show almost a linear dependence of β with the pump power, clear evidence of two-photon nonlinear processes.²² Here we observe neither saturation nor bleaching of absorption. Indeed the absorption at 813 nm is extremely weak or even negligible.⁸ In addition, the laser energy ($\hbar\omega$) we used meets the two-photon absorption condition,¹⁴ $E_{g2} < 2\hbar\omega < 2E_{g2}$, where E_{g2} is the optical band gap.⁸ Figure 2 shows a well-defined bell shaped minimum transmittance at the focus. All these features are suggesting two-photon absorption as the origin of the nonlinear absorption.

By comparing $\text{Re } \chi^{(3)}$ and $\text{Im } \chi^{(3)}$ one can conclude that $\text{Re } \chi^{(3)} \gg \text{Im } \chi^{(3)}$, that is the nonlinearity is mostly refractive. The absolute values of $\chi^{(3)} = [(\text{Re } \chi^{(3)})^2 + (\text{Im } \chi^{(3)})^2]^{1/2}$ are significantly larger than the bulk Si values ($\sim 6 \times 10^{-12}$ esu)^{17,26} and are of the same orders of magnitude as those reported for porous silicon⁴ and for glasses containing nanocrystallites.^{18,20} In the literature the sign and magnitude of $\chi^{(3)}$ for Si-nc formed by ion implantation or laser ablation vary significantly with respect to size, wavelength of the pump, pump power, and laser pulse duration.^{21,22} However, we have not observed any change in the sign of $\chi^{(3)}$ with respect to pump power (Fig. 3) while its absolute value shows a significant Si-nc size dependence (Fig. 4). Moreover our values are close to those expected theoretically for low dimensional Si materials.^{23,24}

The increase of $\chi^{(3)}$ with respect to bulk values in the low dimensional semiconductor is attributed to several mechanisms.^{19,27-30} Among them, only the intraband transitions are expected to be size dependent, as they originated from modified electronic transitions by the quantum confinement effects.¹⁹ Hence the $\chi^{(3)}$ increase is mainly due to quantum confinement.

Quantum confinement effects on $\chi^{(3)}$ have been estimated in several works.^{24,27-30} Theoretical attempts were

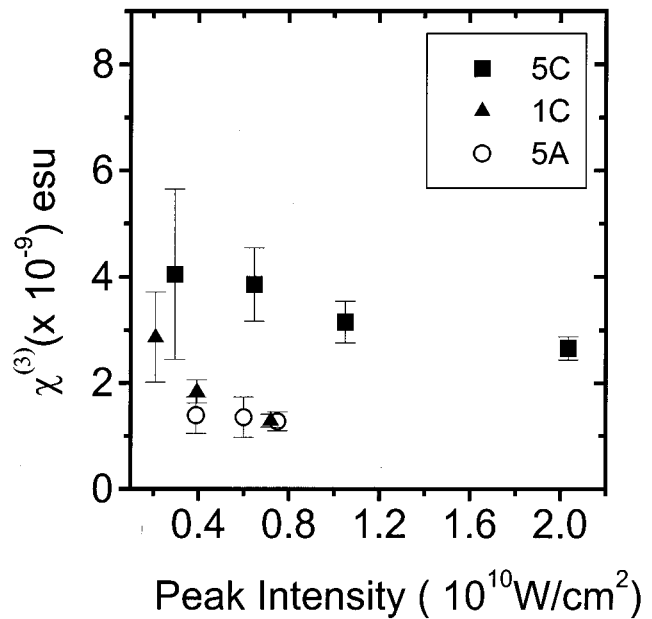


FIG. 3. Absolute values of nonlinear optical susceptibilities $\chi^{(3)}$ at different peak power intensities for Si-nc in SiO_2 films.

made to study *p*-Si as one-dimensional quantum wire and for nonresonant excitation conditions.^{24,27} It was found that the increase in the oscillator strengths caused by the confinement-induced localization of excitons originates from the increase of $\chi^{(3)}$. In fact, the exciton Bohr radius a_0 decreases with the size of quantum wires with respect to the bulk value and hence $\chi^{(3)}$ sensitively increases proportionally to $(1/a_0)$.⁶ The estimated $\chi^{(3)}$ for *p*-Si is close to the measured value for *p*-Si in Ref. 27 and slightly larger than what we measured and other reported values.⁴ The dependence of $\chi^{(3)}$ on Si-nc radius r is plotted in Fig. 4. The increase in $\chi^{(3)}$ is not as sharp as expected by the theoretical

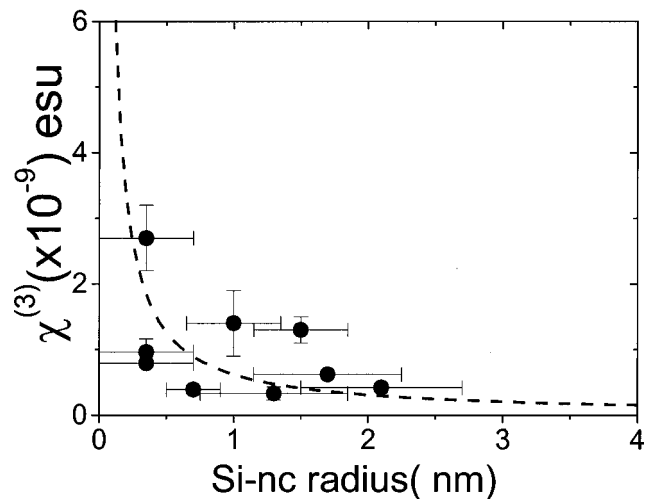


FIG. 4. Variation of $\chi^{(3)}$ with Si-nc radius r . r were determined by TEM measurements and the horizontal error bar corresponds to the width of the Si-nc size distribution. Data have been taken from this work and Ref. 25. All the data have been taken at a peak intensity of $\sim 10 \text{ GW/cm}^2$. Dashed line is a fit with $\chi^{(3)} = \chi_{\text{bulk}}^{(3)} + A/r + B/r^2$.

model, but follows more closely $\chi_{\text{Si-nc}}^{(3)} = \chi_{\text{bulk}}^{(3)} + A/r + B/r^2$. It should be noted that a similar polynomial dependence is theoretically expected for the size dependence of the emission energies of Si-nc (Ref. 8) and the theory of Refs. 24 and 27 is not for Si-nc but for Si quantum wires. In reality, the experimentally determined $\chi^{(3)}$ is related to the microscopic $\chi_m^{(3)}$ by $\chi^{(3)} = p \cdot |f|^4 \chi_m^{(3)}$, where p is the volume fraction and f is a local field correction that depends on the dielectric constant of embedded matrix and nanocrystals.¹⁹ Hence, in addition to r other parameters such as effective refractive index and volume fraction of Si-nc in the embedded matrix should also be taken into account.²⁹ This could explain the scatter in the data of Fig. 4. A direct comparison of $\chi^{(3)}$ values measured here with those for the Si-nc prepared by other methods is difficult because of significant variation in the preparation method, Si-nc size, wavelength of the pump laser, and pump power.^{5-7,21,22} Moreover, the size dependence was not observed earlier and our article reports on an attempt to correlate the nonlinear optical properties with the Si-nc sizes.

In conclusion, the sign and magnitude of both real and imaginary parts of third-order nonlinear susceptibility $\chi^{(3)}$ of Si-nc grown by PECVD have been determined by the Z-scan technique performed at 813 nm with a femtosecond laser. A distinct positive nonlinearity is observed for all these samples. A variation of $\chi^{(3)}$ values with respect to the Si-nc size is reported and related to quantum confinement effects. These results are quite encouraging for nonlinear applications of PECVD grown silicon nanocrystals.

This work has been supported by MURST through Project No. COFIN 99 (MODESTI) and by INFN through the project RAMSES. The authors thank Mr. Salvo Pannitteri (CNR-IMETEM) for TEM analysis and Dr. S. Venugopal Rao (University of St. Andrews) for discussions.

¹O. Bisi, S. Ossicini, and L. Pavesi, *Surf. Sci. Rep.* **38**, 1 (2000).

²J. Linnros, in *Silicon Based Microphotonics: From Basics to Applications*, edited by O. Bisi, S. U. Campisano, L. Pavesi and F. Priolo (IOS, Netherlands, 1999), p. 47.

- ³W. H. Lee, B. R. Taylor, and S. M. Kauzari, in *Proceedings of OSA Technical Digest*, Washington, 2000 p. 12.
- ⁴F. Z. Henari, K. Morgenstern, W. J. Blau, V. A. Karavanski, and V. S. Dneprovskii, *Appl. Phys. Lett.* **67**, 323 (1995) and references therein.
- ⁵S. Vijaya Lakshmi, F. Shen, and H. Grebel, *Appl. Phys. Lett.* **71**, 3332 (1997).
- ⁶S. Vijaya Lakshmi, M. A. George, and H. Grebel, *Appl. Phys. Lett.* **70**, 708 (1997).
- ⁷E. Borsella *et al.*, *Mater. Sci. Eng.*, B **79**, 55 (2001).
- ⁸G. Vijaya Prakash *et al.*, *J. Nanosci. Nanotech.* **1**, 159 (2001).
- ⁹F. Iacona, G. Franzò, and C. Spinella, *J. Appl. Phys.* **87**, 1295 (2000).
- ¹⁰F. Priolo, G. Franzò, D. Pacifici, V. Vinciguerra, F. Iacona, and A. Irrera, *J. Appl. Phys.* **89**, 264 (2001).
- ¹¹M. Sheik-Bahae, A. A. Said, and E. W. Van Stryland, *Opt. Lett.* **14**, 955 (1989).
- ¹²M. Sheik-Bahae, A. A. Said, T.-H. Wei, D. J. Hagan, and E. W. Van Stryland, *IEEE J. Quantum Electron.* **26**, 760 (1990).
- ¹³P. P. Ho and R. R. Alfano, *Phys. Rev. A* **20**, 2170 (1979).
- ¹⁴Y. R. Shen, *The Principles of Nonlinear Optics* (Wiley, New York, 1984), p. 202.
- ¹⁵A. Hache and M. Bourgeois, *Appl. Phys. Lett.* **77**, 4089 (2000).
- ¹⁶D. H. Reitze, T. R. Zang, Wm. M. Wood, and M. C. Downer, *J. Opt. Soc. Am. B* **7**, 84 (1990).
- ¹⁷J. F. Reintjes and J. C. McGroddy, *Phys. Rev. Lett.* **30**, 901 (1973).
- ¹⁸M. Murayama and T. Nakayama, *Phys. Rev. B* **49**, 5737 (1994); **52**, 4986 (1995).
- ¹⁹J. M. Ballesteros, J. Solis, R. Serna, and C. N. Afonso, *Appl. Phys. Lett.* **74**, 2791 (1999).
- ²⁰E. M. Vogel, M. J. Weber, and D. M. Krol, *Phys. Chem. Glasses* **32**, 231 (1991).
- ²¹S. Vijaya Lakshmi, H. Grebel, Z. Iqbal, and C. W. White, *J. Appl. Phys.* **84**, 6502 (1998).
- ²²S. Vijaya Lakshmi, H. Grebel, G. Yaglioglu, R. Pino, R. Dorsinville, and C. W. White, *J. Appl. Phys.* **88**, 6418 (2000).
- ²³J. Wang, H.-b. Jiang, W.-C. Wang, J.-B. Zheng, F.-L. Zhang, P.-H. Hao, X.-Y. Hou, and X. Wang, *Phys. Rev. Lett.* **69**, 3252 (1992).
- ²⁴R. Chen, D. L. Lin, and B. Mendoza, *Phys. Rev. B* **48**, 11879 (1993).
- ²⁵G. Vijaya Prakash, M. Cazzanelli, Z. Gaburro, F. Iacona, G. Franzò, F. Priolo, and L. Pavesi, *J. Mod. Opt.* (in press).
- ²⁶J. J. Wynne, *Phys. Rev.* **178**, 1295 (1969).
- ²⁷S. Lettieri, O. Fiore, P. Maddalena, D. Ninno, G. Di Francia, and V. La Ferrara, *Opt. Commun.* **168**, 383 (1999).
- ²⁸S. Schmitt-Rink, D. A. B. Miller, and D. S. Chemla, *Phys. Rev. B* **35**, 8113 (1987).
- ²⁹E. Hanamura, *Phys. Rev. B* **37**, 1273 (1988).
- ³⁰D. Cotter, M. G. Burt, and R. J. Manning, *Phys. Rev. Lett.* **68**, 1200 (1992).